J Mol Model (2011) 17:721–726
DOI 10.1007/s00894-010-0774-9

ORIGINAL PAPER

Self-assembled monolayers of oligosilane on the silicon (001) surface: molecular dynamics simulations

Li Zhao · Xue-Mei Duan · Xiang-Gui Xue · Ming-Hui Li · Ze-Sheng Li

Received: 6 March 2010 / Accepted: 28 May 2010 / Published online: 10 June 2010

Abstract Atomistic molecular dynamics simulations have been used to investigate the adsorption of permethyldecasilane (MS10) on the silicon (001) surface. The condition under which the self-assembled monolayer forms is examined. The properties of the well-ordered structures, including the packing patterns, the equilibrium distances between two neighboring chains, and the tilt angles, are calculated to characterize the structure of the self-assembled monolayer. The results are comparable with those obtained experimentally.

Keywords Self-assembled monolayer · Oligosilane · Molecular dynamics simulations

Introduction

Conjugated molecules have received considerable attention in recent years due to their wide range of possible applications. They can be used in active electronic and optoelectronic organic materials such as light-emitting diodes, polymer lasers, photovoltaic cells, field-effect transistors, photoconductors, and electroluminescent devices. Si-based polymers and oligomers that possess σ-conjugated electrons that are delocalized along the silicon main chains have attracted much interest among the wide range of conjugated polymer systems available because of their unusual photophysical and electronic properties [1–11], especially their relatively high hole mobilities [12–17]. Compared with polysilanes, oligosilanes have definite silicon chain lengths and hence well-defined σ-conjugated lengths, and thus the relationship between the structures and the interesting properties of these polymers should be studied [16, 17].

Most properties of conjugated molecules are anisotropic with respect to the main chain axis, so the molecular conformation and the intermolecular packing are important for understanding their interesting properties and for effectively utilizing those properties to design optical and electronic devices. Many oligosilane systems with well-ordered structures have been prepared and studied by different experimental techniques. Kaito and co-workers prepared highly oriented films of permethyloligosilanes by the vacuum-deposition method and studied their properties by X-ray diffraction, low-wavenumber Raman scattering, infrared spectroscopy and ultraviolet absorption spectroscopy [18, 19]. They also reported that the films showed liquid-crystalline properties [20, 21]. Tamao and Tsuji showed a powerful way to control the conformation along a linear oligosilane chain unambiguously in their recent papers [22–26]. Krempner and co-workers studied well-defined oligosilane dendrimers in the nanometer regime, which was useful for understanding the photophysical properties of silicon nanostructures [27–30].

Although many experimental studies have been performed to explore the structures of oligosilanes and their unique properties, there are still some problems to solve, such as the detailed packing structure of the molecules. Take the linear permethyldecasilane ($Me(SiMe_2)_{10}Me$) prepared by vacuum-deposition for example [31]: two types of highly ordered structures, one with its molecules oriented normal to the substrate and the other with an oblique orientation, were found in $Me(SiMe_2)_{10}Me$ films deposited at room temperature using X-ray diffractometry and absorption spectroscopy

L. Zhao · X.-M. Duan · X.-G. Xue · M.-H. Li · Z.-S. Li (✉)
State Key Laboratory of Theoretical and Computational Chemistry, Institute of Theoretical Chemistry, Jilin University, Changchun 130023, People's Republic of China
e-mail: zeshengli@mail.jlu.edu.cn

with a varying angle of incidence to the substrate. The precise tilt angle and the reason why there are two types of structures remain uncertain. Molecular dynamics (MD) simulation is a powerful theoretical tool for investigating this type of problem because it provides atomic-level information [32].

In this study, an attempt is made to examine whether the well-ordered SAM of $Me(SiMe_2)_{10}Me$ (MS10) can be produced on the silicon (001) surface. Our interest focused on the range of average area per chain within which a well-ordered SAM would form. The structure of the monolayer is characterized by the packing pattern, the equilibrium distance between two neighboring chains, and the tilt angles. The results are compared with those obtained experimentally. We hope that our simulation provides useful structural information that can help us to understand the basic properties of conjugated oligosilanes. Details of the MD simulation are presented in the next section, followed by the results obtained from it and a discussion of them, and then conclusions.

Model and simulation method

All of the studies were performed using the Discover module in the Material Studio 3.1 commercial modeling software package from Accelrys Inc. [33]. A 3-D periodic box was employed in the MD simulations. MS10 chains along the *Z*-axis were embedded into the simulation box with the fixed silicon surface parallel to the *XY* plane. The silicon (001) surface, cleaved from a silicon crystal with lattice constants $a=b=c=5.42$ Å and $\alpha=\beta=\gamma=90°$, is a 7×7 superstructure with a thickness of around 12 Å. All chains were built perpendicular to the surface initially. Figure 1 shows a typical initial conformation with a chain number of 12 and an average area per chain of 44.23 $Å^2$. The length of the simulation box in the *Z*-direction was enlarged to 80 Å, which is large enough to allow us to ignore the interactions between MS10 chains and the periodic images of the surface in the top plane. The 3-D periodicity inherent in the model is transformed into an actual 2-D periodicity to simulate an infinitely extended surface.

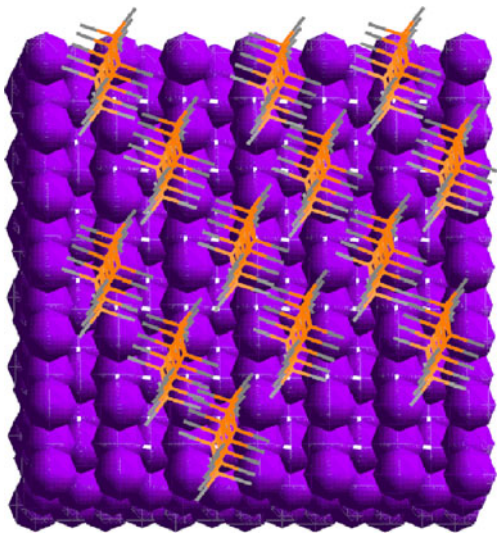

Fig. 1 Initial conformation of MS10-13 on the silicon (001) surface. H atoms of chains are ignored for clarity

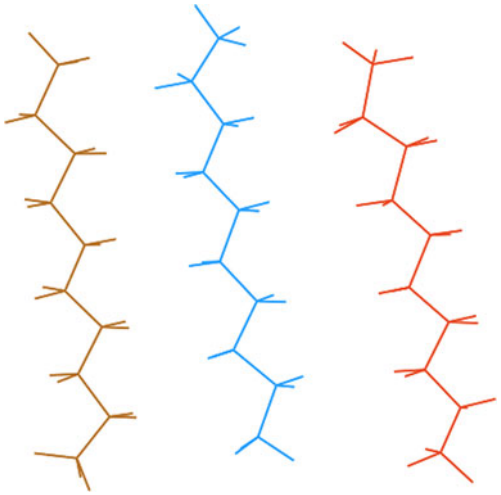

Fig. 2 Snapshot of MS10-3 (top view). Different chains are depicted in different colors. H atoms of the chains and the silicon surface are ignored for clarity

The MD simulations were performed according to the following procedures. The simulations of each system using different initial chain positions were performed three times to ensure the reliability of the results. Firstly, energy minimization was carried out to relax the local unfavorable structure. Then a 2 ns MD simulation was performed for every system using the COMPASS force field [34–37]. The number of chains used in each simulation ranged from 1 to 14. The notation MS10-*n* ($n=1–14$) was used to denote the models. The van der Waals interactions were calculated with a cutoff $r_c=12$ Å and a spline function from 11 Å. Coulomb interactions were calculated via Ewald summation [32]. A canonical (NVT) ensemble was adopted, and the equation of motion was integrated with a time step of 0.001 ps. The temperature was controlled through the Berendsen thermostat [38] with a relaxation time of 0.1 ps.

Results and discussion

The results for the structure of MS10 at 300 K will be discussed in this section. All simulations ran until the total and potential energies fluctuated around a constant value, indicating that equilibrium had been reached.

The prime motivation for our simulation study was to determine the critical condition under which the well-

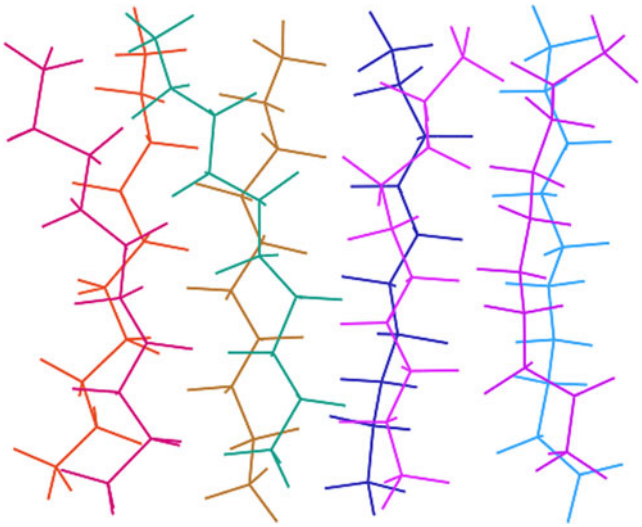

Fig. 3 Snapshot of MS10-8 (side view). Different chains are depicted in different colors. H atoms of the chains and the silicon surface are ignored for clarity

ordered SAM would form. Simulations of MS10-*n* (*n*=1–14), representing different average areas per chain, were carried out. The results are divided into four parts, according to the final structure of the chains on the surface in the equilibrium state. Firstly, for *n*=1–3, the chains in the models are all parallel to the surface. However, different initial structures lead to different equilibrium packing patterns. Well-ordered structures are not obtained. A typical snapshot of MS10-3 is shown in Fig. 2. Secondly, the chains in the models tilt with different tilt angles on the surface when *n* ranges from 4 to 9. Well-ordered structures are not found under this condition, as shown in Fig. 3. Thirdly, and most importantly, for *n*=10–13, corresponding to an average area per chain of 53.07–40.82 Å^2, the chains in the box are parallel to each other and have almost identical tilt angles. They form well-ordered structures. The important optical and electrical properties of the conjugated oligomers are based on their well-ordered structures, and it has been reported that the molecular axes of MS10 are perpendicular to the layer planes in vacuum-deposited films and the liquid crystal phase [18–21], so we have largely focused on such systems. Typical snapshots of MS10-12 and MS10-13 are shown in Fig. 4. Finally, when the value of *n* equals 14, one chain in the model is squeezed out of the monolayer plane while the others are perpendicular to the surface. It can be concluded that the saturated number of chains in one monolayer is 13, corresponding to an average area per chain of 40.82 Å^2. If more chains are put into a monolayer, some of them are extruded out, leaving at most 13 chains. Structural properties, including packing patterns, tilt angles, and stability as functions of the average area per chain, will be discussed in the following.

Snapshots of MS10 models with chains that are highly oriented on the surface in the equilibrium state are shown in

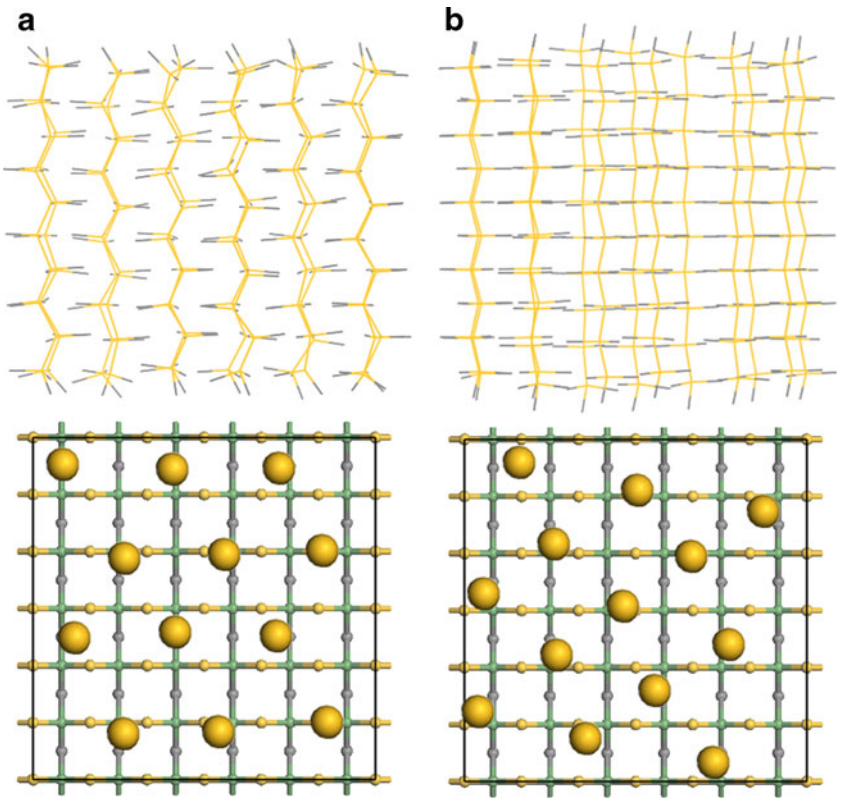

Fig. 4 **a**–**b** Snapshots of MS10-*n* with *n*=12 (**a**) and *n*=13 (**b**). The *upper and the lower snapshots* correspond to the side and the top views, respectively. In the upper snapshots, the silicon surface and the H atoms of the chains are ignored. In the bottom snapshots, the *big yellow balls* denote the centers of mass of the chains and the *small balls* denote surface atoms, where the *yellow*, the *green* and the *gray balls* denote the first-, the second- and the third-layer atoms, respectively

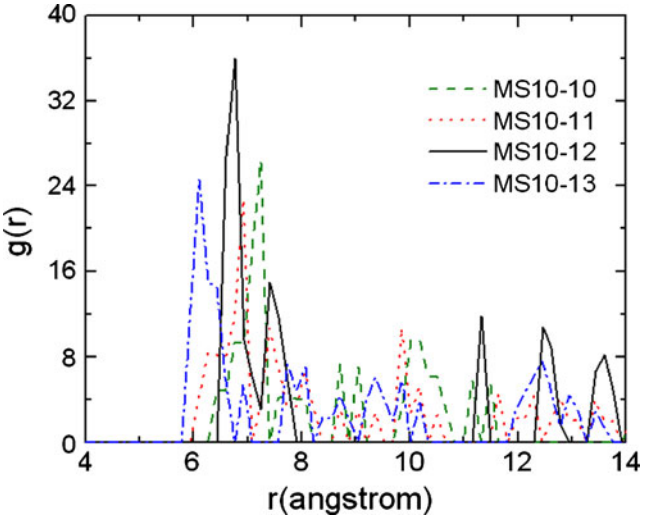

Fig. 5 Modified radial distribution functions of the center of mass for MS10-*n* (*n*=10, 11, 12 and 13)

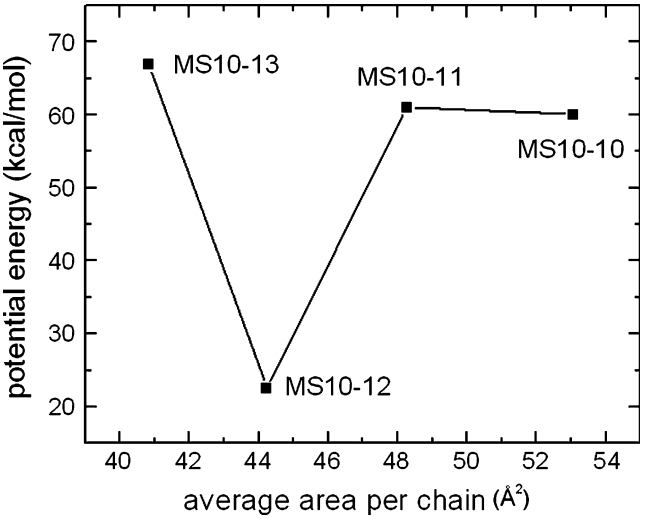

Fig. 6 The potential energy of MS10-*n* (*n*=10, 11, 12 and 13)

Fig. 4. For brevity, only typical structures are displayed, i. e., the structures of MS10-12 and -13 denoted "a" and "b" in Fig. 4, respectively. The reason for choosing these two snapshots is that MS10-13 and MS10-12 have the highest and the lowest energies, respectively. A discussion of the stability of MS10-*n* (*n*=10–13) will be given on the basis of the potential energy in the following. The upper snapshots in Fig. 4 present side views of the models. They show that all of the chains are parallel to each other with identical tilt angles between the main chains and the silicon surface. The bottom snapshots in Fig. 4 present top views of the models. The big yellow balls in the regular array denote the positions of the centers of mass of the chains in the *XY* plane. It is worth noting that, taken together, the big yellow balls yield a structure with a deformed hexagonal symmetry and a high degree of order. In addition, there was no apparent relationship between the centers of mass of the chains and the surface sites, as shown in Fig. 4. However, the hexagonal symmetry of MS10-12 in Fig. 4a is more regular than those of the others. Hexagonal symmetry can also be found in the liquid crystal phase of MS10 within the layer plane [20].

Table 1 The average areas and tilt angles averaged over all chains of MS10-*n* (*n*=10, 11, 12 and 13)

MS10-*n*	Average area per chain (Å^2)	Tilt angles (degrees)
MS10-13	40.82	84.90
MS10-12	44.23	85.32
MS10-11	48.25	84.55
MS10-10	53.07	70.09

The classical radial distribution function (RDF) is modified to yield the equilibrium distance between two neighboring chains in the monolayer, namely the side length of the hexagon in Fig. 4. The new RDF is defined as follows: it gives a measure of the probability that, given the presence of a center of mass of a chain at the origin of an arbitrary reference frame, there will be a center of mass of a chain located in a spherical shell of infinitesimal thickness at a distance *r* from the reference silicon. Plots of the new RDFs, given in Fig. 5, show not only the exact value of the equilibrium distance between two neighboring chains but also the degree of order of the monolayer. It is known that the higher the first peak, the higher the degree of order. It is clear that the structure of MS10-12 is more regular than the others. This result is in accord with that shown in Fig. 4.

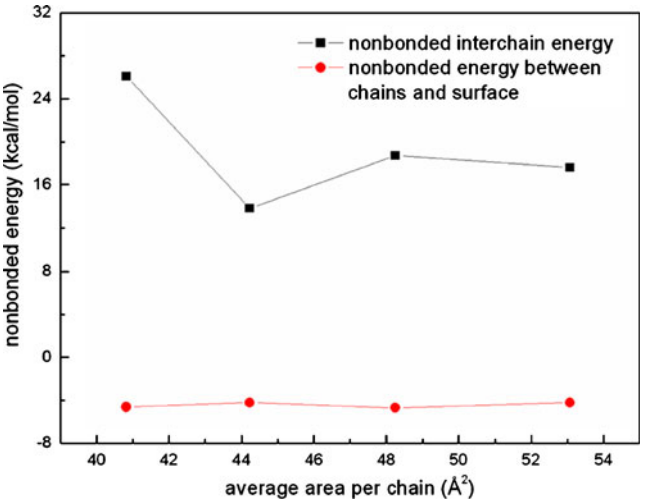

Fig. 7 The nonbonded energy of MS10-*n* (*n*=10, 11, 12 and 13). The *red squares* denote the interchain nonbonded energy and the *black circles* denote the nonbonded energy between the chains and the surface

The equilibrium side length of the hexagon, namely the equilibrium distance between two neighboring chains, is 7.53, 7.07, 6.27 and 5.92 Å for MS10-10, 11, 12 and 13, respectively.

Tilt angles between the vectors of the main chain and the silicon surface are calculated to characterize the chain tilt on the surface. Their values are shown in Table 1. There are virtually only two values: one is about 70.09°, when the average area per chain is 53.07 Å, and the other is about 84.92°, which is the average value of the tilt angles when the average area per chain ranges from 48.25 to 40.82 Å. This result is comparable with that observed for MS10 in vacuum-deposited film [33], where two types of structure are seen, one with molecules perpendicular to the surface and the other with an oblique orientation. The reason why there are two types of tilt angle will be discussed on the basis of potential energy in the following.

The potential energy averaged over all chains (referred to as the "potential energy" from hereon) is calculated to compare the stabilities of the systems in our MD simulations. The potential energy decreases gradually at first during the simulation process, and then fluctuates within a small range. The drop in the potential energy corresponds to the process where the chains adjust their positions and tilt angles to achieve a regular arrangement and suitable conditions in the monolayer. The values of the equilibrium energy, averaged over the final 500 ps, are shown in Fig. 6. It can be concluded that MS10-12 is the most stable configuration because it has the lowest potential energy. Further, MS10-10, MS10-11 and MS10-13 appear to be stable configurations because their potential energies are comparable with that of MS10-12. This may explain the existence of two tilt angles, as mentioned above. Moreover, the interchain nonbonded energies and the nonbonded energies between the chains and the surface were calculated and are presented in Fig. 7. The nonbonded energy was averaged across all chains. Figure 7 shows that the interchain nonbonded energy displays a similar behavior to the potential energy, while the nonbonded energy between the chains and the surface fluctuates around a constant value. Therefore, the self-assembling behavior of the monolayer appears to depend mainly on the interchain interaction.

For MS10-n ($3<n<10$), a well-ordered SAM could not be obtained because the attractive forces between the surface and the chains were too strong. The average distance between two neighboring chains increases as the number of chains in the simulation box decreases. The chains tilt on the surface to achieve a balance between the attractive and repulsive forces among the chains.

In the study of MS10-n ($n\leq3$), all of the chains are adsorbed parallel to the surface. The attractive force between the chains and the surface is much stronger than that among the chains, so the chains are arranged randomly on the surface. The equilibrium positions of the chains are mainly determined by their initial positions. We tried to place more chains parallel to the surface initially, but the extra chains are squeezed, causing them to tilt on the surface.

Conclusions

In the present study, molecular dynamics simulation was employed to investigate the structure details of MS10 physisorbed onto a silicon (001) surface at 300 K. We found that a stable self-assembled monolayer could form when the average area per chain ranged from 40.82 to 53.07 $Å^2$. The chains in the monolayer were almost perpendicular to the surface and parallel to each other. Well-ordered packing structures with hexagonal symmetry were obtained. We hope that our results may aid the material design of silicon-based oligomeric compounds due to the particular importance of molecular orientation and packing in thin films.

Acknowledgments This work was supported by the National Science Foundation of China (20933001, 20973049).

References

1. Miller RD, Michl J (1989) Chem Rev 89:1359–1410
2. Takashi K (2008) J Photochem Photobiol C 9:111–137
3. Crespo R, Piqueras MC, Michl J (2007) Theor Chem Acc 118:81–87
4. Sasaki M, Shibano Y, Tsuji H, Araki Y, Tamao K, Ito O (2007) J Phys Chem A 111:2973–2979
5. Tachikawa H, Kawabata H (2007) J Organomet Chem 692:1511–1518
6. Krempner C, Kockerling M (2008) Organometallics 27:346–352
7. Nespurek S, Wang G, Yoshino K (2005) J Optoelectron Adv Mater 7:223–230
8. Tang HD, Liu YY, Huang B, Qin JG, Fuentes-Hernandez C, Kippelen B, Li SJ, Ye C (2005) J Mater Chem 15:778–784
9. Acharya A, Seki S, Saeki A, Tagawa S (2006) Synth Met 156:293–397
10. Saxena A, Rai R, Kim SY, Fujiki M, Naito M, Okoshi K, Kwak G (2006) J Polym Sci Polym Chem 44:5060–5075
11. Li MJ, Qiu HY, Jiang JX, Lai GQ, Feng SY (2007) J Appl Polym Sci 104:2445–2450
12. Kepler RG, Zeigler JM, Harrah LA, Kurtz SR (1987) Phys Rev B 35:2818–2822
13. Abkowitz M, Bässler H, Stolka M (1991) Philos Mag B 63:201–220
14. Bässler H, Borsenberger PM, Perry RG (1994) J Polym Sci B Polym Phys 32:1677–1685
15. Okumoto H, Yatabe T, Shimomura M, Kaito A, Minami N, Tanabe Y (2001) Adv Mater 13:72–76
16. Okumoto H, Yatabe T, Richter A, Peng JB, Shintomura M, Kaito A, Minami N (2003) Adv Mater 15:716–720
17. Sasaki M, Shibano Y, Tsuji H, Araki Y, Tamao K, Ito O (2007) J Phys Chem A 111:2973–2979

18. Yatabe T, Shimomura M, Kaito A (1996) Chem Lett 551–552
19. Shimomura M, Yatabe T, Kaito A, Tanabe Y (1997) Macromolecules 30:5570–5571
20. Yatabe T, Kaito A, Tanabe Y (1997) Chem Lett 799–800
21. Yatabe T, Suzuki Y, Kawanishi Y (2008) J Mater Chem 18:4468–4477
22. Tamao K, Tsuji H, Terada M, Asahara M, Yamaguchi S, Toshimitsu A (2000) Angew Chem Int Ed 39:3287–3290
23. Tsuji H, Terada M, Toshimitsu A, Tamao K (2003) J Am Chem Soc 125:7486–7487
24. Tsuji H, Fukazawa A, Yamaguchi S, Toshimitsu A, Tamao K (2004) Organometallics 23:3375–3377
25. Mallesha H, Tsuji H, Tamao K (2004) Organometallics 23:1639–1642
26. Fukazawa A, Tsuji H, Tamao K (2006) J Am Chem Soc 128:6800–6801
27. Krempner C, Jäger-Fiedler U, Köckerling M, Ludwig R, Wulf A (2006) Angew Chem Int Ed 45:6755–6759
28. Krempner C, Reinke H (2003) J Organomet Chem 685:134–137
29. Krempner C, Chtchian S, Reinke H (2004) Inorg Chim Acta 357:3733–3738
30. Krempner C, Köckerling M, Mamat C (2006) Chem Commun 7:720–722
31. Ichino Y, Minami N, Yatabe T, Obata K, Kira M (2001) J Phys Chem B 105:4111–4117
32. Allen MP, Tildesley DJ (1978) Computer simulation of liquid. Clarendon, Oxford
33. Accelrys Software, Inc. (2004) Materials Studio: getting started, release 3.1. Accelrys Software, Inc., San Diego
34. Sun H (1995) Macromolecules 28:701–712
35. Sun H (1998) J Phys Chem B 102:7338–7364
36. Sun H, Ren P, Fried JR (1998) Comput Theor Polym Sci 8:229–246
37. Rigby D, Sun H, Eichinger BE (1997) Polym Int 44:311–330
38. Berendsen HJC, Postma JPM, Gunsteren WF, DiNola A, Haak JR (1984) J Chem Phys 81:3684–3690